Frequency spectrum analysis on the force contribution in a micronewton electromagnetic thruster

D.S.H. Charrier[*,†]

[*]Institut P` (CNRS – Université de Poitiers – ENSMA), UPR 3346, SP2MI – Téléport 2, Bd Marie et Pierre Curie, BP 30179, 86962 Futuroscope, France

[†]Nexans Research Center, 29 rue Pré Gaudry, 69007 Lyon, France

A frequency analysis on results published in 2012 is given in this letter, where experimental displacements of the coil-disc device obtained at different generator square signal frequencies (from 100 Hz to 15 MHz) are compared with monochromatic AC currents calculated from RL and RLC_{stray} circuit impedances. In time domain, a square signal can be decomposed in sum of monochromatic (Dirac-like) contributions in frequency domain. The analysis revealed that i) the RL circuit has a working device onset frequency above 170 kHz ii) the stray capacitance C_{stray} of the coil must be much below the order of pF for having working coil-disc device frequencies. The onset frequency at 170 kHz is coherent with a previous prediction, the device having decimeter scale d at maximum, the monochromatic working threshold frequency was found at about $f_{th} = c/d \approx 3$ GHz.

[*] dimitri.charrier@nexans.com

In 2012, experimental results were reported on an electromagnetic thruster[1] although a similar original concept was reported before by Goodwin.[2,3] Since then, the order of magnitude of thrust or at least the proof-of-principle on a laboratory scale device were not reported by other works. The thrust was explained by an electromagnetic momentum emitted by the coil transferred into mechanical momentum on the metallic disc. Transient regime, asymmetrical coil-disc device, Joule heating accompanying eddy currents helped in creating a total net force and not only on short time scales. In this letter, different physical and theoretical aspects are given to complement past experiments that could help experimentalists willing to reproduce the proof-of-principle and a frequency signal analysis is reported. The force equation was proposed and confronted to experimental results with a relative success:

$$F_{disc} = \frac{1}{t}\int_0^{r_2}\left(2\pi r B_{\rho 1}\int \vec{B}_{z1} d\vec{S}_2 \,/L_2\right)dr$$

Equation 1

where t, r_2, r, $B_{\rho 1}$, B_{z1}, S_2 and L_2 are respectively, the disc thickness, the disc and integration radius, the radial and axial magnetic field components at the extremity of the coil, the disc area and the ring integration inductance. Experiments were performed with an angle between the geological north-sourth line and the coil axis at 15°. The disc was oriented to the south-east and the coil to the north-west. Measurements were performed at Latitude: 46.66 and Longitude: 0.36. A magnetic field component (along B_{z1}) such as the Earth magnetic field which is not time dependent within the time scale of experiments does not create a force on the disc since only the time dependent fields contribute into the force of Equation 1. The issue of surrounding environment of the coil-disc system contributing to the total thrust might be raised when taking into account sources of artifacts, such as mirror charging effects. A care was taken in order to prevent proximity mirror effects by using an immediate environment made of wood.

Recently, works were published on either advices[4] or recommendations[5] for measuring respectively micronewton or even nanonewton. In Ref[1], optical fibers placed in the vicinity of a metal plate collected reflected light. It was shown that the reflected light is linearly proportional to the fiber to metal plate distance in a certain range of distance.[6] The link between collected light and displacement was done using a calibration curve: input reflected light voltage versus displacement in micrometer measured with a micrometer screw. Regarding the acquisition of displacements, the following procedure was followed: acquisition at rest position, a pause of acquisition just before switching on the power supply, few seconds of waiting time, acquisition again. The few seconds of waiting time of displacement acquisition was necessary due to the too high displacement provoked by the first square shape ramps up of the signal. This minor note about the transient regime does not change the displacement observed in the steady regime which was used for the analysis. Therefore all the data as shown in [1] do not show few seconds of displacement after the power supply was switched on. Moreover, complementary trials were performed where the two optical fiber sensors were placed in opposite direction in such way that all artifacts between the coil-disc device and the measurement setup was uncorrelated. Regarding the model and the interpretation of the results, several comments are given here. As proposed by Lafleur[7], the need to consider the speed of sound is of interest when looking at the force establishment on the whole body. The calculations proposed in here[8] were to consider the total force at a time t without regarding any mechanical steady state or relativistic effect. Since the total motion of the rigid or elastic body under non-uniform acceleration is also source of intense investigations, as referenced by Franklin[9] and Dmitriev[10], no further model was built. As shown in Table *1*, the measurement setup and the device characteristics can be decomposed in different frequency spectrum. The terms 'monochromatic' and 'polychromatic' refer respectively to Dirac-like frequency and rich Fourier decomposed frequency spectrum. The thrust measurement setup was composed by pendulum and sampling frequencies. Both are monochromatic. The oscillating frequency of the pendulum $f_p = \sqrt{g/h}/2\pi$ = 1,71 Hz with g the standard gravitational constant (9,81 m s^{-2}) and h the pendulum height (8,5 cm) is crucial when working a low generator square wave frequency. To be relevant, the generator frequency must be at least two times higher than the pendulum oscillating frequency. At low frequency the system coil hung on the pendulum might enter into resonant oscillations. The sampling frequency f_s was about 10 Hz. The data of displacements done with a generator frequency above $2f_s$ = 20 Hz were relevant. As shown in Table *1*, the coil was excited with a square wave generator where the periodic wave is monochromatic and the Fourier decomposed square signal is necessary polychromatic. From the disc side, both working device electromagnetic wave frequencies and eddy current and skin depth frequencies are polychromatic.

In order to identify the unknown working frequency of the device, complementary calculations in frequency domain are presented. The calculations presented in Ref [1] used a linear and resistive ramp up to calculate the current and its derivative as function of time. Here the RL circuit is treated rather than simple resistive R circuit. Then the Equation 2 was used to calculate the current.

$$U = R_{coil} i + L_{coil} \frac{di}{dt}$$

Equation 2

where U, i, R_{coil} and L_{coil} are respectively the voltage, current, resistance and inductance of the coil. Taking conditions of i_{coil}(t=0) = 0 and $\tau = L_{circuit}/R_{circuit}$ then both current and its derivative can be calculated as a function of time as shown in Equation 3, Equation 4 and in Figure 1.

$$i_{coil} = \frac{U}{R_{circuit}} \left(1 - exp\left(-\frac{t}{\tau}\right)\right)$$

Equation 3

$$\frac{di_{coil}}{dt} = \frac{U}{L_{circuit}} exp\left(-\frac{t}{\tau}\right)$$

Equation 4

In frequency domain, the RL circuit is described using the impedance terms as shown in Equation 5:

$$Z_{RL} = R_{coil} + jL_{coil}\omega$$

Equation 5

where ω is equal et $2\pi f$ with the f the frequency of the signal. Using the norm of impedance, it is possible to use the impedance to deduce the current flowing in the coil in one single frequency,

$$i_{coil} = \frac{U}{|Z_{RL}|} = \frac{U}{\sqrt{R_{coil}^2 + L_{coil}^2\omega^2}}$$

Equation 6

Using the frequency domain, the derivative d$i_{coil}(\omega)$/dt is equal at zero.

Inductances are known to behave as capacitor at high frequencies because the presence of isolated spires influence themselves. As shown in Figure 2, the stray capacitance coming from the inductance is added in the impedance calculations. The impedance term is shown in Equation 7.

$$Z_{RLCstray} = \frac{\left(R_{coil}^2 + L_{coil}^2\omega^2\right)\left[R_{coil} - j\omega\left(C_{stray}R_{coil}^2 + C_{stray}L_{coil}^2\omega^2 - L_{coil}\right)\right]}{R_{coil}^2 + \omega^2\left(C_{stray}R_{coil}^2 + C_{stray}L_{coil}^2\omega^2 - L_{coil}\right)^2}$$

Equation 7

where C_{stray} is the stray capacitance that is to be defined. Impedance terms contrarily to Equation 3 and Equation 4 allow a frequency-domain study rather than a time-domain study. As shown in Figure 3, according to the stray capacitance values (RLC circuit), the current in the coil has a minimum while in the case of RL circuit the current decreases with the frequency. In Figure 4, the experimental and calculated displacements are shown. The experimental displacement was obtained with the so-called polychromatic square wave generator while the calculated displacements are monochromatic coming from the impedance terms. The aim of this representation is to identify the working monochromatic frequencies. For instance, in the case of stray capacitance of value 1 pF, less than two decades of frequencies are involved in the displacement while in the case of RL or RLC with 1 fF, a large working frequency spectrum is identified above 170 kHz (~1,8 km wavelength). Electromagnetic momentum transfer into mechanical momentum in the disc is possible using a continuum spectrum of Dirac-like frequencies above 170 kHz. Indeed frequencies below 170 kHz are not playing a role in the force. This observation is consistent with what it has been proposed in the past[8]. In term of experimental improvements, the exciting signal must be monitored accurately in order to extract the full Fourier decomposed spectrum. The same spectrum can be inserted in the calculation and confronted to experiments. The force can be increased by decreasing the resistivity of disc, using low temperatures. Stray capacitance can be reduced by replacing N spires into a single large flat metal sheet or using electronic means of compensation.

Figure captions:

Figure 1: Current i and its derivative di/dt in time domain in the RL device circuit.

Figure 2: Equivalent circuit of the operational device under electromagnetic excitation. Stray capacitance between the coil spires changes the device response.

Figure 3: Currents calculations in monochromatic frequency domain using RL and RLC impedances (1 nF and 1 pF stray capacitances).

Figure 4: Real displacement as produced by a polychromatic square wave generator (Fourier decomposition of a square contains infinity a monochromatic frequencies) versus monochromatic calculated displacements.

Tables:

Table 1 : Decomposition of frequencies present in the experiments reported in Ref [1].

References

[1] D.S.H. Charrier, Appl. Phys. Lett. **101**, 034104 (2012).

[2] D.P. Goodwin, AIP Conf. Proc. **552**, 976 (2001).

[3] D.P. Goodwin, AIP Conf. Proc. **699**, 1175 (2004).

[4] J. Soni and S. Roy, Rev. Sci. Instrum. **84**, 095103 (2013).

[5] J.E. Polk, A. Pancotti, T. Haag, S. King, M. Walker, J. Blakely, and J. Ziemer, in *33rd Int. Electr. Propuls. Conf.* (2013), pp. 1–24.

[6] C. Coupeau, J.C. Girard, and J. Grilhé, J. Vac. Sci. Technol. B Microelectron. Nanom. Struct. **16**, 1964 (1998).

[7] T. Lafleur, Appl. Phys. Lett. **105**, 146101 (2014).

[8] D.S.H. Charrier, Prog. Electromagn. Res. M **13**, 69 (2010).

[9] J. Franklin, Found. Phys. **43**, 1489 (2013).

[10] A.L. Dmitriev, AIP Conf. Proc. **969**, 1163 (2008).

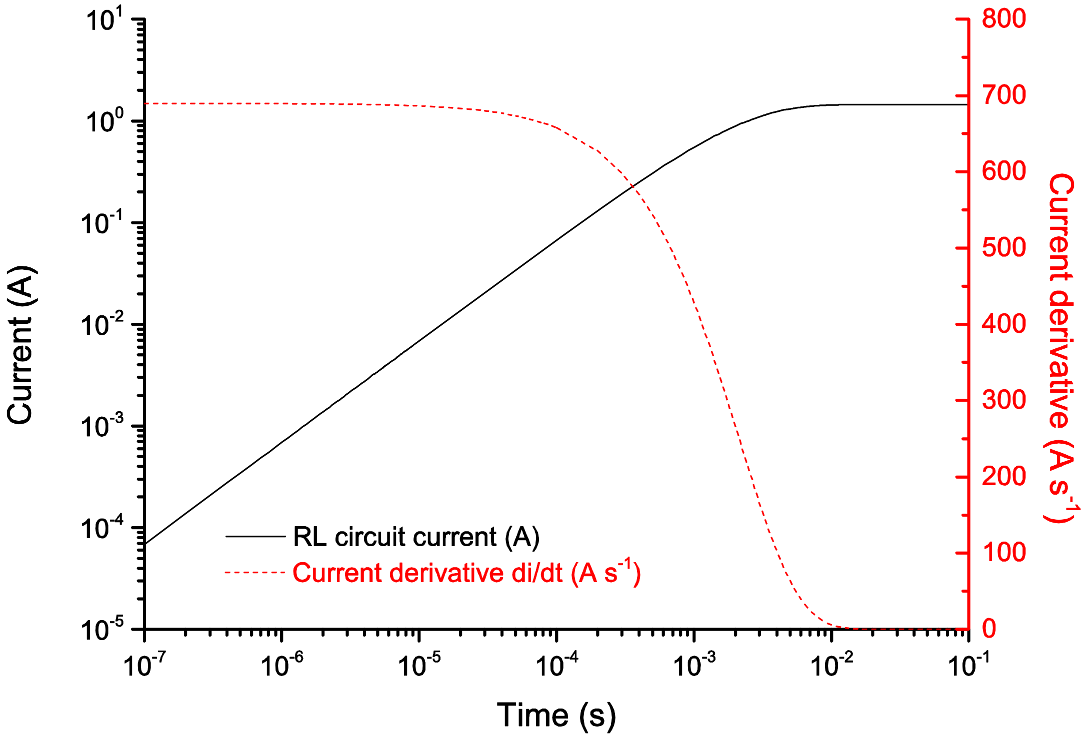

Current (A)
Current derivative (A s^{-1})
Time (s)
RL circuit current (A)
Current derivative di/dt (A s^{-1})

FIGURE 1

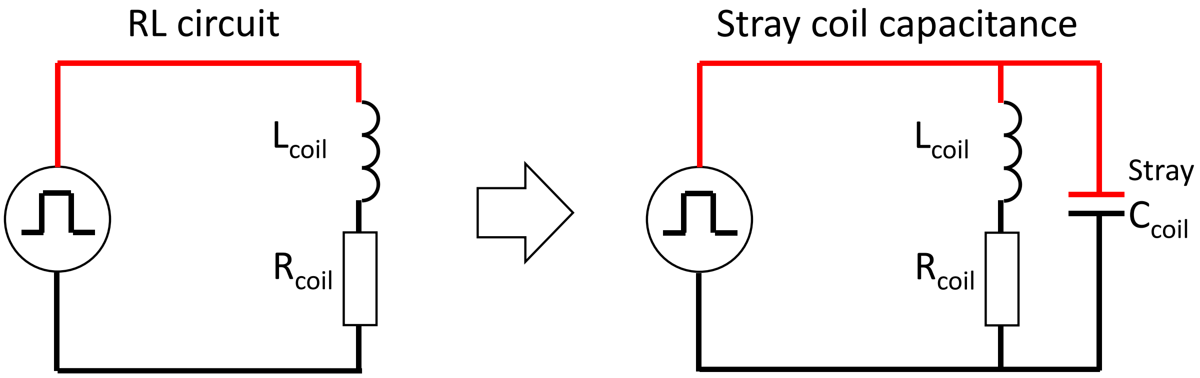
RL circuit
Lcoil
Rcoil
Stray coil capacitance
Lcoil
Rcoil
Stray
Ccoil

FIGURE 2

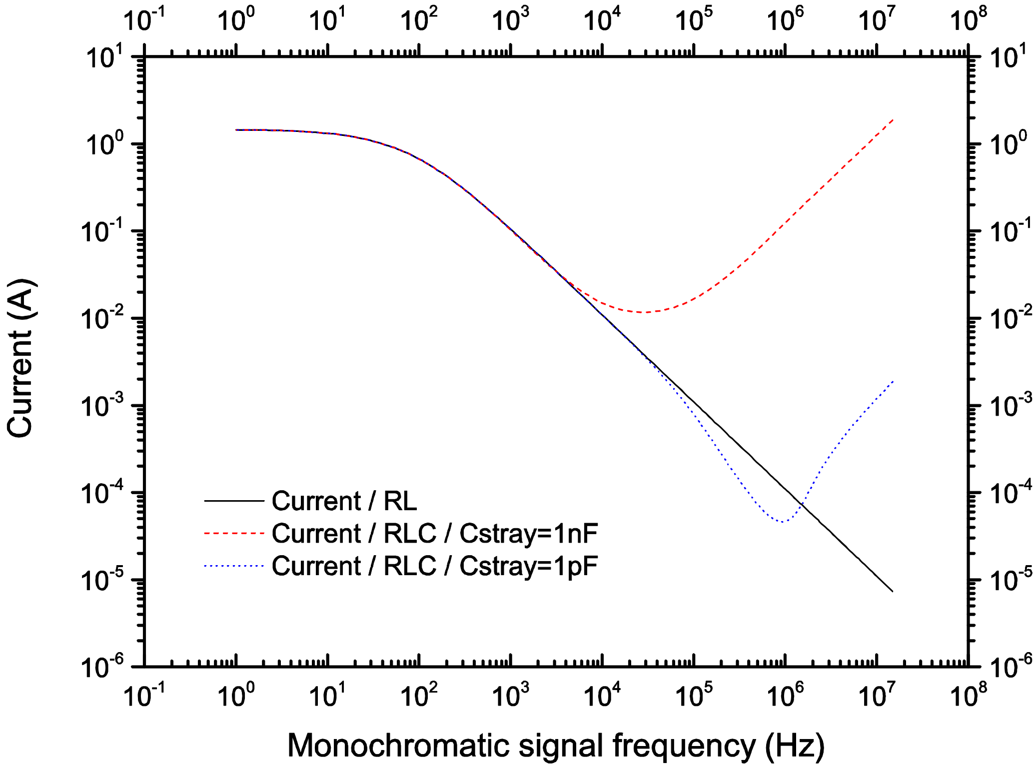
Current (A)
Monochromatic signal frequency (Hz)
Current / RL
Current / RLC / Cstray=1nF
Current / RLC / Cstray=1pF
10^-1
10^0
10^1
10^2
10^3
10^4
10^5
10^6
10^7
10^8
10^-6
10^-5
10^-4
10^-3
10^-2

FIGURE 3

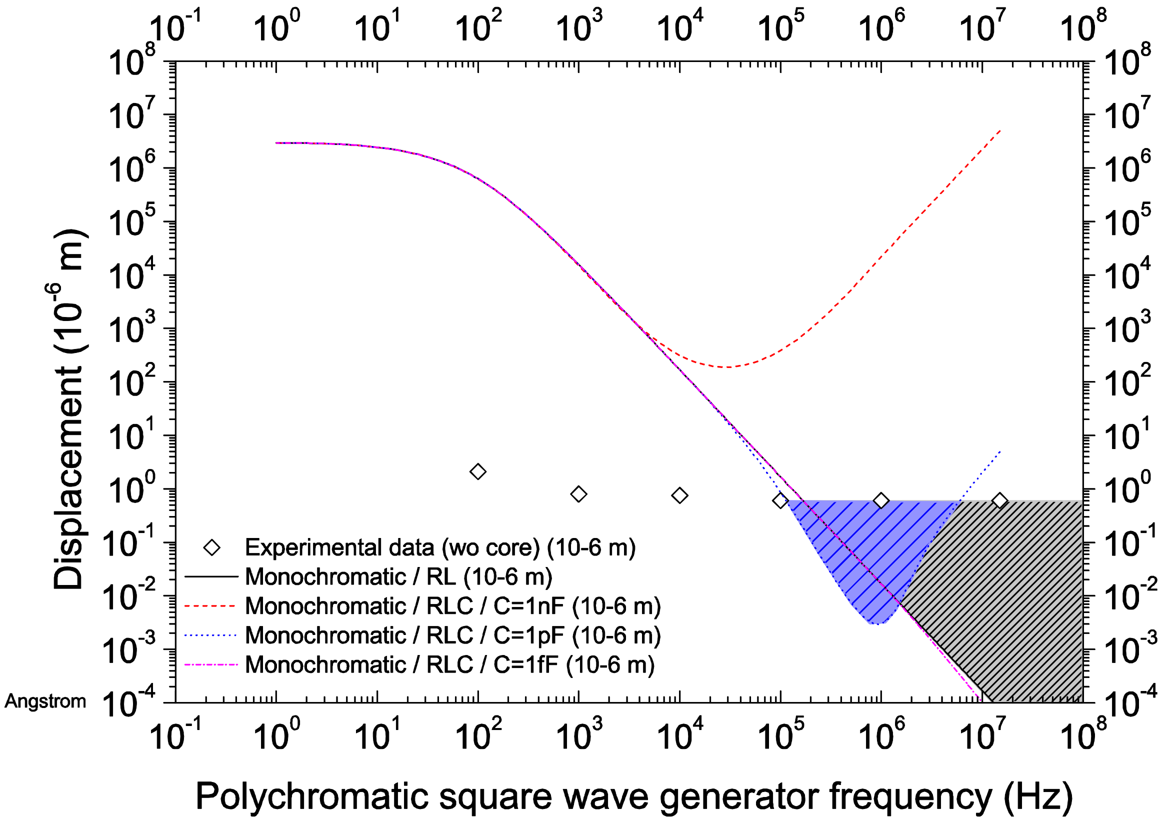

Displacement (10^{-6} m)
Polychromatic square wave generator frequency (Hz)
Angstrom
Experimental data (wo core) (10-6 m)
Monochromatic / RL (10-6 m)
Monochromatic / RLC / C=1nF (10-6 m)
Monochromatic / RLC / C=1pF (10-6 m)
Monochromatic / RLC / C=1fF (10-6 m)

FIGURE 4

	Frequency (Hz)	Spectrum	Status in the model
Thrust measurement setup	Pendulum frequency	Dirac	Known
	Sampling frequency	Dirac	Known
Emitter coil	Generator square wave frequency	Dirac	Known
	Fourier frequencies in a single square wave	Continuum	Not measured
Receptor disc	Working device electromagnetic wave frequencies	Continuum	Unknown
	Eddy currents and skin depth with frequencies	Continuum	Not quantified

TABLE 1